ORNL/TM-2015/651

Oak Ridge National Laboratory Active-Well Counting Using New "PSD-Plastic" Detectors

Paul A. Hausladen
Robert D. McElroy
Jason Newby

November 2015

OAK RIDGE NATIONAL LABORATORY
MANAGED BY UT-BATTELLE FOR THE US DEPARTMENT OF ENERGY

DOCUMENT AVAILABILITY

Reports produced after January 1, 1996, are generally available free via US Department of Energy (DOE) SciTech Connect.

Website http://www.osti.gov/scitech/

Reports produced before January 1, 1996, may be purchased by members of the public from the following source:

National Technical Information Service
5285 Port Royal Road
Springfield, VA 22161
Telephone 703-605-6000 (1-800-553-6847)
TDD 703-487-4639
Fax 703-605-6900
E-mail info@ntis.gov
Website http://www.ntis.gov/help/ordermethods.aspx

Reports are available to DOE employees, DOE contractors, Energy Technology Data Exchange representatives, and International Nuclear Information System representatives from the following source:

Office of Scientific and Technical Information
PO Box 62
Oak Ridge, TN 37831
Telephone 865-576-8401
Fax 865-576-5728
E-mail reports@osti.gov
Website http://www.osti.gov/contact.html

This report was prepared as an account of work sponsored by an agency of the United States Government. Neither the United States Government nor any agency thereof, nor any of their employees, makes any warranty, express or implied, or assumes any legal liability or responsibility for the accuracy, completeness, or usefulness of any information, apparatus, product, or process disclosed, or represents that its use would not infringe privately owned rights. Reference herein to any specific commercial product, process, or service by trade name, trademark, manufacturer, or otherwise, does not necessarily constitute or imply its endorsement, recommendation, or favoring by the United States Government or any agency thereof. The views and opinions of authors expressed herein do not necessarily state or reflect those of the United States Government or any agency thereof.

ORNL/TM-2015/651

Nuclear Security and Isotope Technology Division

Active-Well Counting Using New "PSD-Plastic" Detectors

P. A. Hausladen, R. D. McElroy, J. Newby

Date Published: November 2015

Prepared by
OAK RIDGE NATIONAL LABORATORY
Oak Ridge, TN 37831-6283
managed by
UT-BATTELLE, LLC
for the
US DEPARTMENT OF ENERGY
under contract DE-AC05-00OR22725

CONTENTS

LIST OF FIGURES iv
ACRONYMS AND ABBREVIATIONS vi
ABSTRACT 1
1. INTRODUCTION 1
2. THEORY OF OPERATION 3
3. DESCRIPTION OF THE EQUIPMENT 4
4. PROOF OF PRINCIPLE MEASUREMENTS 8
   4.1 Detector Characterization 8
   4.2 Measurements of Uranium Standards 11
   4.3 Predicted performance of the PSD Plastic compared to the AWCC 13
5. MULITPLE-SCATTERING SYSTEMATICS 15
6. SUMMARY 20
7. REFERENCES 20

LIST OF FIGURES

Figure 1. The "PSD-plastic" fast-neutron imaging system used for the present work as viewed from (left) the side and (right) the back with the covers removed. 5
Figure 2. A segmented detector (upper left) showing the array of PSD-plastic, (upper right) combined with the thermal-neutron detector, and (below) assembled for insertion in the housing. 5
Figure 3. The (left) position response of a detector to uniform illumination by fast neutrons, and (right) pulse shape response to a combination of gamma rays, fast neutrons, and thermal neutrons. 6
Figure 4. The imager with the source holder designed specifically for this work, and (right) a cutaway of the sleeve showing the sleeve, the ^{241}Am(Li) plugs, and the mounting of the sources internal to the sleeve. 7
Figure 5. Photograph of the AWCC sleeve mounted in front of the PSD-plastic detector panel. 7
Figure 6. Estimated singles and non-adjacent doubles efficiencies based on detector solid angle and an intrinsic efficiency of 0.18. 8
Figure 7. Comparison of measured and calculated (left) singles and (right) non-adjacent doubles efficiencies. The singles measurements indicate that at close distances there is noticeable loss in efficiency due to coincidence summing with fission gamma rays. 9
Figure 8. The distributions of (left) neutron singles and (right) neutron-scatter doubles for an ^{241}Am(Be) source positioned at the middle of the AWCC sleeve. 9
Figure 9. The distribution of neutron doubles in distance (1 pixel = 1.08 cm) and time for an ^{241}Am(Be) source (upper left) and a ^{252}Cf source (upper right) where half the rate-corrected ^{241}Am(Be) distribution is subtracted from the ^{252}Cf distribution. By accepting only doubles above the red line, the multiple scattering contribution is limited while maintaining good efficiency for fission neutron doubles. The efficiency and fraction of singles from ^{241}Am(Be) that produce a double are plotted (lower left) as the y-intercept of the cut (red line) is varied to minimize the statistical uncertainty for the largest mass (lower right). 10
Figure 10. The PSD-plastic measured doubles rates of the ^{235}U standards are presented as a function of ^{235}U mass. A rational function of the form $\mathrm{DF} = \mathrm{Am}/(1 + \mathrm{Bm})$ is fit to each curve. A second curve (dotted) was fit to the fast mode data and is described in the text. 13
Figure 11. Proposed Reconfigured Detector. 14
Figure 12. The performance of the AWCC and PSD-plastic operated in "fast mode" with two interrogating sources in each end plug each with activity of 5×10^4 neutrons·s^{-1}. Also, shown is the predicted performance for a reconfigured PSD-plastic system with four times the singles efficiency and with interrogating activities scaled by a factor of 10. 15
Figure 13. The relative error as a function of the ^{241}Am(Li) source strength. 15
Figure 14. Energy deposition distribution for Backgrounds, Am(Be), AmLi(+Bckgd), and AmLi Only. 16
Figure 15. The doubles distributions over spatial and time separation within the detector plane for ^{241}Am(Be), ^{241}Am(Li), and ^{252}Cf. The center "AmLiOnly" plot is a subtraction of the ambient background distribution from the ^{241}Am(Li) dataset. The "Cf–AmBe" distribution is the estimated true fission doubles distribution obtained by subtracting half the single-neutron-rate scaled ^{241}Am(Be) distribution from the ^{252}Cf distribution. 17
Figure 16. The doubles distribution collected for 13.5 h of 181 g of ^{235}U is fit by subtracting the duration scaled Ambient+AmLi distribution and the fission (Cf-AmBe) distribution, and multiple-scattering [^{241}Am(Be)] distributions are allowed to vary. The 2D residuals (in counts and sigma) are shown on the left, and three slices in time-difference of the distributions are shown on the right. 18

Figure 17. The doubles distribution collected for 13.5 h of 181 g of ^{235}U is fit by subtracting the duration scaled Ambient+AmLi distribution and the fission (Cf-AmBe) distribution, and multiple-scattering [^{241}Am(Li)] distributions are allowed to vary. The 2D residuals (in counts and sigma) are shown on the left, and three slices in time-difference of the distributions are shown on the right. 19
Figure 18. Comparison of the corrected doubles rate with the doubles rate from fitting the 2D doubles distributions. 20

ACRONYMS AND ABBREVIATIONS

AWCC	Active Well Coincidence Counter
HEU	highly enriched uranium
LEU	low enriched uranium
PMT	photomultiplier tube
PSD	plastic scintillation detector
UNCL	Uranium Neutron Coincidence Collar

ABSTRACT

This report presents results and analysis from a series of proof-of-concept measurements to assess the suitability of segmented detectors constructed from an Eljen EJ-299-34 "PSD-plastic" scintillator with pulse-shape discrimination capability for the purpose of quantifying uranium via active neutron coincidence counting. Present quantification of bulk uranium materials for international safeguards and domestic materials control and accounting relies on active neutron coincidence counting systems, such as the Active Well Coincidence Counter (AWCC) and the Uranium Neutron Coincidence Collar (UNCL), that use moderated ^{3}He proportional counters along with necessarily low-intensity ^{241}Am(Li) neutron sources. Scintillation-based fast-neutron detectors are a potentially superior technology to the existing AWCC and UNCL designs due to their spectroscopic capability and their inherently short neutron coincidence times that largely eliminate random coincidences and enable interrogation by stronger sources. One of the past impediments to the investigation and adoption of scintillation counters for the purpose of quantifying bulk uranium was the commercial availability of scintillators having the necessary neutron-gamma pulse-shape discrimination properties only as flammable liquids. Recently, an Eljen EJ-299-34 "PSD-plastic" scintillator became commercially available. The present work is the first assessment of an array of PSD-plastic detectors for the purposes of quantifying bulk uranium. The detector panel used in the present work was originally built as the focal plane for a fast-neutron imager, but it was repurposed for the present investigation by construction of a stand to support the inner well of an AWCC immediately in front of the detector panel. The detector panel and data acquisition of this system are particularly well suited for performing active-well fast-neutron counting of low-enriched uranium and highly enriched uranium samples because the active detector volume is solid, the ^{241}Am(Li) interrogating neutrons are largely below the detector threshold, and the segmented construction of the detector modules allow for separation of true neutron-neutron coincidences from inter-detector scattering using the kinematics of neutron scattering. The results from a series of measurements of a suite of uranium standards are presented and compared to measurements of the same standards and source configurations using the AWCC. Using these results, the performance of the segmented detectors reconfigured as a well counter is predicted and outperforms the AWCC.

1. INTRODUCTION

The quantitative assay of bulk uranium and plutonium materials in international safeguards applications has traditionally been carried out using moderate to high efficiency (in this case $\epsilon > 10\%$) but relatively slow thermal neutron coincidence assay systems. At present, the Uranium Neutron Collar (UNCL) and the Active Well Coincidence Counter (AWCC) provide quantitative mass analysis of bulk uranium items by means of active neutron interrogation and neutron coincidence counting. In both cases, the measurements suffer from poor signal-to-noise ratios and require long assay times to achieve the desired measurement precision. However, the same assays may be accomplished using less efficient but faster scintillation detection systems while providing significant improvements in measurement precision.

As an example, the AWCC consists of an annular geometry neutron detector composed of moderated ^{3}He proportional counters along with ^{241}Am(Li) neutron sources that fit in plugs on either end of the well [1]. It works by detecting coincident neutrons emitted from fissions of ^{235}U stimulated by neutrons from the sources. The use of ^{241}Am(Li) for the interrogating sources is suitable for this task because the energy of the emitted neutrons is insufficient to fission ^{238}U, and the source neutrons themselves are not correlated (not coincident). Consequently, the number of coincident neutrons is roughly proportional to ^{235}U mass. The main limitation in measuring the rate of coincident neutrons in the AWCC is the large random coincident rate due to neutrons from the interrogating source. In fact, the rate of random coincidences limits the "useful" strength of the interrogating source that can be employed since larger sources will not improve the signal to noise.

Scintillation-based fast-neutron detectors are a potentially superior technology to the existing AWCC and UNCL designs due to their spectroscopic capability and their inherently short neutron coincidence times that largely eliminate random coincidences and enable interrogation by stronger sources. One of the past impediments to the investigation and adoption of scintillation counters for the purpose of quantifying bulk uranium was the commercial availability of scintillators having the necessary neutron-gamma pulse-shape discrimination properties only as flammable liquids. Recently, Eljen EJ-299-34 "PSD-plastic" scintillator with pulse-shape discrimination capabilities has become available.

In the present work, we evaluate an existing array of PSD-plastic detectors for the purposes of quantifying bulk uranium. The detector panel used in the present work was originally built by Oak Ridge National Laboratory (ORNL) as the focal plane for a fast-neutron imager, but it was repurposed for the present investigation by construction of a stand to support the inner well of an AWCC immediately in front of the detector panel. The detector panel consists of 16 segmented detector modules (each a 10 × 10 array of square pixels 1.08 cm on a side and 5 cm in length) with an intrinsic detection efficiency of approximately 20%. As configured for these evaluation measurements, the detection efficiency for fission neutrons emitted from the sample item was approximately 5%. The detector panel and data acquisition of this system are particularly suited for performing active well fast-neutron counting of low-enriched uranium (LEU) and highly enriched uranium (HEU) samples for the following reasons:

- The active volume is solid, not liquid, and will not leak or degrade from gradual oxygenation.
- The efficiency of these detectors remains approximately constant for neutron energies between 2 MeV to 6 MeV but falls to almost 0 below energies of 750 keV [2].
- When used with ^{241}Am(Li) interrogation, almost all the interrogating neutrons are below threshold in the detector and will not contribute to the fast-neutron rate. This allows the counting of fast neutrons of energies greater than the ^{241}Am(Li) (α, n) neutrons, dramatically reducing the random uncertainty contributions from the interrogation source.
- The data acquisition uses commercially available waveform digitizers: Struck 3316 250 megasample per second (MSs^{-1}) 14-bit digitizers with a compact, high-density form factor.
- The segmented construction of the detector modules allows optimal suppression of inter-detector scatter using the kinematics of neutron scattering.

Remarkably, the performance of this existing, non-optimized, single detector slab approximately equals the performance of the traditional AWCC system. From the results, we conclude that a coincidence counter comprising multiple PSD-plastic detectors in an optimized geometry will far exceed the measurement performance of these traditional counters, enabling significantly reduced assay times or increased precision. The fast-neutron detector assemblies will also provide additional information related to timing and coincidence multiplicities that may afford improved accuracy to identify unexpected material configurations (e.g., item spiking with a spontaneous fission source).

This report opens with a discussion of the statistical errors for counting with the AWCC and the corresponding statistical errors using PSD detectors. Then, the PSD-plastic detector and its configuration as a well counter are described, followed by a description of the proof-of-concept measurements of uranium standards. The uranium standards results are analyzed to predict the precision of the measurements over a range of uranium masses, both for the present detector configuration as well as a higher efficiency configuration. These results are compared to identical measurements using an AWCC. Last of all, further analysis is performed to extract the number of true coincidences and inter-detector scatter coincidences with high confidence.

2. THEORY OF OPERATION

The purpose of active-well coincidence counting is to measure the number of true fission coincidences, which are then related to the ^{235}U mass. In this section, we relate the rates of true and accidental coincidences to parameters such as the interrogating source strength, and form expressions for the statistical uncertainty of the measurements. In this way, the uncertainty for a broad range of potential measurements can be predicted from the limited number of measurements performed in the present work with available sources.

First, we consider the various rates that statistically limit the AWCC driven by a ^{241}Am(Li) source [1]. Throughout this work, we focus only on the contributions of random statistical uncertainties to the measurement precision. In the limit of negligible environmental backgrounds, the total number of doubles observed in the well counter is

$$D = D_F + D_{Acc},$$

where D is the rate of measured doubles within a coincidence time window G from fission (D_F) and uncorrelated accidentals (D_{Acc}) from a total measured singles rate of S. These rates depend on the rate of fissions Φ_I, the rate of singles from fissions (S_F), and the rate of singles neutrons (S_α) from the interrogating source of intensity, I_α,

$$\begin{gathered}\Phi_F = P(m)I_\alpha \\ S_F = \nu_1\epsilon_S\Phi_F \\ S_\alpha = \epsilon_\alpha I_\alpha \\ D_F = \eta\epsilon_S^2\nu_2 P(m)I_\alpha \\ S = I_\alpha(\nu_1\epsilon_S P(m) + \epsilon_\alpha) \\ D_{Acc} = S^2 G\end{gathered}$$

where ϵ_α is the efficiency for detecting a neutron from the interrogating source, $P(m)$ is the probability that an interrogating neutron induces a fission, ϵ_S is the efficiency for a fission neutron, and ν_1 and ν_2 are the mean number of neutrons and neutron pairs emitted from an induced fission. The efficiency for detecting a second correlated neutron is less than detecting a single neutron by some fraction (η) due to either dead-time or finite time gating, so the efficiency for a correlated double is $\epsilon_D \equiv \eta\epsilon_S^2$.

The uncertainty on the rate of doubles from fissions is then given by

$$\sigma_{D_F}^2 = \frac{D_F + 2S^2G}{\mathrm{t}}.$$

Similarly, the time (t) to a specified relative precision (σ_{D_F}/D_F) is

$$\mathrm{t} = \frac{1}{\sigma_{\mathrm{D_F}}^2/D_F^2}\frac{\mathrm{D_F} + 2\mathrm{S}^2\mathrm{G}}{D_F^2}.$$

In situations where the accidentals from the driving source dominate the error ($2\mathrm{S}^2\mathrm{G} \gg \mathrm{D_F}$), the time is

$$t = \frac{2G}{\sigma_{\mathrm{D_F}}^2/D_F^2}\left(\frac{\epsilon_\alpha}{\eta\nu_2 P(m)\epsilon_S^2}\right).$$

The fast-neutron well counter analysis is similar to that of the AWCC, but there are a couple of key differences to consider. First, for the AWCC, the activity of the interrogating source is chosen such that the factor $\mathrm{G} \times \mathrm{S} \approx 1$. In contrast, the same interrogating source activity will yield a typical value of $\mathrm{G} \times \mathrm{S} < 10^{-6}$ for the fast-neutron system. This difference in magnitude is because the coincidence gate for

fast neutrons can be as small as 30 ns, but also because the fast neutron detectors are largely insensitive to neutrons emitted by the ^{241}Am(Li) source. Second, in the fast-neutron system, there is an additional contribution of error originating from multiply scattered neutrons. Unlike neutron-capture detectors, where each neutron can only be counted once, the fast scintillators used in the present work allow multiple detections. In the scintillation detectors, fast neutrons are detected when they elastically scatter off of hydrogen (protons) in the scintillator, and the recoiling proton creates scintillation light as it stops. As a result, if the same neutron scatters in more than one detector volume, it can be detected more than once. The probability that a fast-neutron will be counted more than once depends on the geometry of the detectors, the scattering material, and on the fast-neutron energy distribution. Since the energy distribution of the interrogating source may differ significantly from the fission neutron energy distribution, we identify the mean number of scatter coincidence counts per fast neutron as ρ_α and ρ_F. The measured rate of doubles for the PSD-plastic system is then

$$D = D_F + D_{Acc} + \rho_F S_F + \rho_\alpha S_\alpha.$$

Since we estimate the rate of accidentals and the rate of fission singles from the measured rate, the statistical uncertainty on the estimate for the fission doubles rate is as follows:

$$\sigma_{D_F}^2 = \frac{1}{t}\left(D + (2SG + \rho_F)^2 S\right)$$

$$\sigma_{D_F}^2 = \frac{1}{t}\left(D_F + S^2G(1 + 4SG + 4\rho_F) + (\rho_F + \rho_F^2)S + (\rho_\alpha - \rho_F)S_\alpha\right)$$

Note that the uncertainty of the rate of accidental doubles from the measurement of the singles rate results in the factor of $2 \rightarrow 1 + 4R_S G$, which for the AWCC would be about 3, but for the fast-neutron system is negligibly different from 1. Let us now consider the relative error:

$$\frac{\sigma_{D_F}^2}{D_F^2} = \frac{1}{t}\left(\frac{1}{D_F} + \frac{S^2G(1 + 4SG + 4\rho_F)}{D_F^2} + \frac{(\rho_F + \rho_F^2)S}{D_F^2} + \frac{(\rho_\alpha - \rho_F)S_\alpha}{D_F^2}\right)$$

It is clear from the previous equation that the uncertainty is minimized as before by minimizing the rate of accidentals, but now also the rate of multiple scattering doubles from both fission neutrons and the interrogating neutrons. Quantifying the contributions of these factors requires estimates of the multiple-scattering rate and the ratio of fission neutron efficiency to the interrogating neutron efficiency for the PSD-plastic detectors. Note also that this analysis assumes that the values of ρ_α and ρ_F are constant and not changed by (for example) scattering in the sample changing the energy of the neutrons.

3. DESCRIPTION OF THE EQUIPMENT

In this section, the detector panel and data acquisition are described. Then, modifications to the system to make it suitable for use as a well counter are described.

As stated earlier, the fast-neutron detector panel used in the present work was repurposed from a fast-neutron imager. Although the imaging system has been described previously [3,4], some details will be repeated here for clarity. The imaging system is shown in Figure 1 with its detector panel and data acquisition labeled.

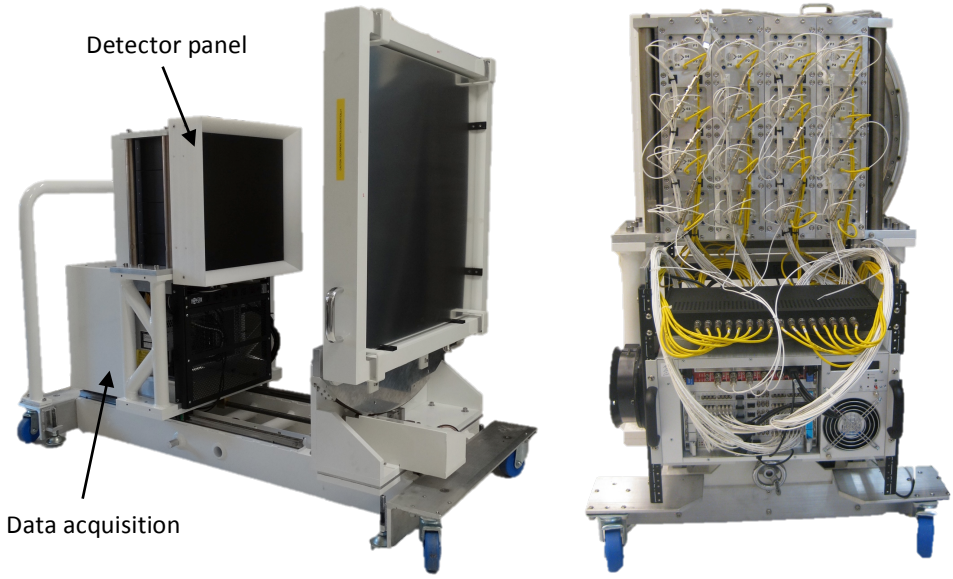

Figure 1. The "PSD-plastic" fast-neutron imaging system used for the present work as viewed from (left) the side and (right) the back with the covers removed.

The detector panel consists of 16 segmented detector modules with intrinsic detection efficiency for fission-spectrum neutrons of approximately 20%. The active volume of a single detector module, typically referred to as the "pixel block," consists of a 10.8 × 10.8 × 5 cm^3 volume of scintillator EJ-299-34 segmented by 3M Vikuiti reflector into a 10 × 10 array of 1.08 × 1.08 × 5 cm^3 optically isolated pixels of plastic scintillator. The pixels are viewed through a 28-mm-thick segmented acrylic light guide by four 52-mm Hamamatsu R7724-100 super bialkali photomultiplier tubes (PMTs) whose shared response determines the pixel of interaction. The detector module is placed in a housing whose external dimensions in the imaging plane are 11.2 cm × 11.2 cm. The detector array is shielded on the front and sides by 6 mm of lead shielding and a further 5 cm of polyethylene shielding on the sides. As a side note, the detectors also include a thermal-neutron phosphor on the front face. However, the thermal-neutron data was not used in the present work. Illustrative photographs of a single detector module as it is assembled are shown in Figure 2.

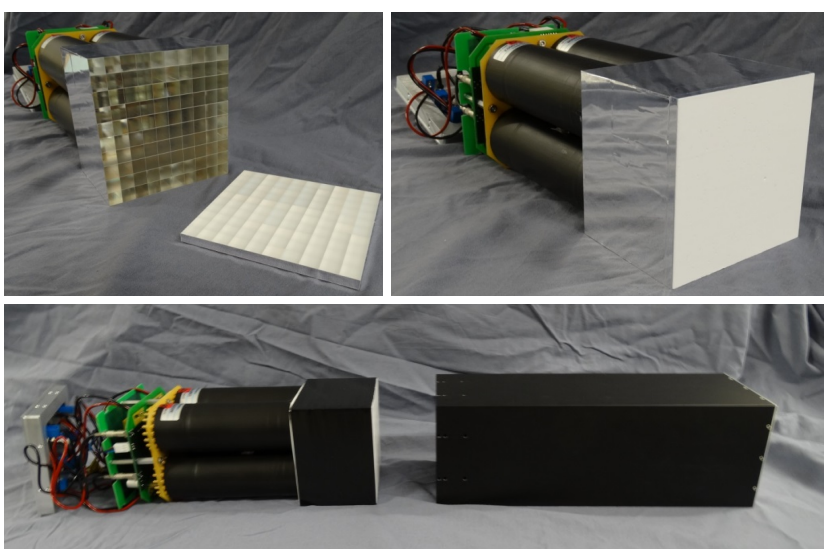

Figure 2. A segmented detector (upper left) showing the array of PSD-plastic, (upper right) combined with the thermal-neutron detector, and (below) assembled for insertion in the housing.

The philosophy behind the data acquisition for the detector panel was to use off-the-shelf hardware in a well-established chassis format. Then, to the extent that was reasonable, data were written to disk in a raw format that enabled detailed offline analysis that could be updated as analysis techniques improved. Toward this end, the data acquisition was based on four Struck SIS3316 250 MSs^{-1} free-running waveform digitizers. When the sum signal from the four PMTs in a detector exceeded a set threshold, a summary of each of the signals was recorded. The individual PMT signals corresponded to tail pulses having a time constant of approximately 2.5 μs, so a summary that included a 200-ns integral of baseline that precedes the pulse followed by samples at 112 ns, 116 ns, 866 ns, and 870 ns after the end of the baseline sample was sufficient to summarize the shape of each pulse. The two earlier samples captured the integral of the fast component of scintillation light, and the two later samples capture the total integral. The ratio of the fast to total was used to calculate the pulse shape, and the relative amount of signal in the four PMTs was used to calculate the position of interaction in the pixel block. The use of sequential pairs of points for the fast component and total integral enabled interpolation between the points to correct for the timing of the pulse with respect to the timing of the digitizer samples. A typical example of the position response of a single detector to uniform illumination by fast neutrons, or a "flood image," is shown on the left of Figure 3. The flood image corresponds to a histogram of the calculated x and y position centroids of each interaction. In this flood image, each of the bright spots corresponds to a detector pixel. In the analysis of the data, the nearest pixel to the calculated position was assigned to each count in the detector.

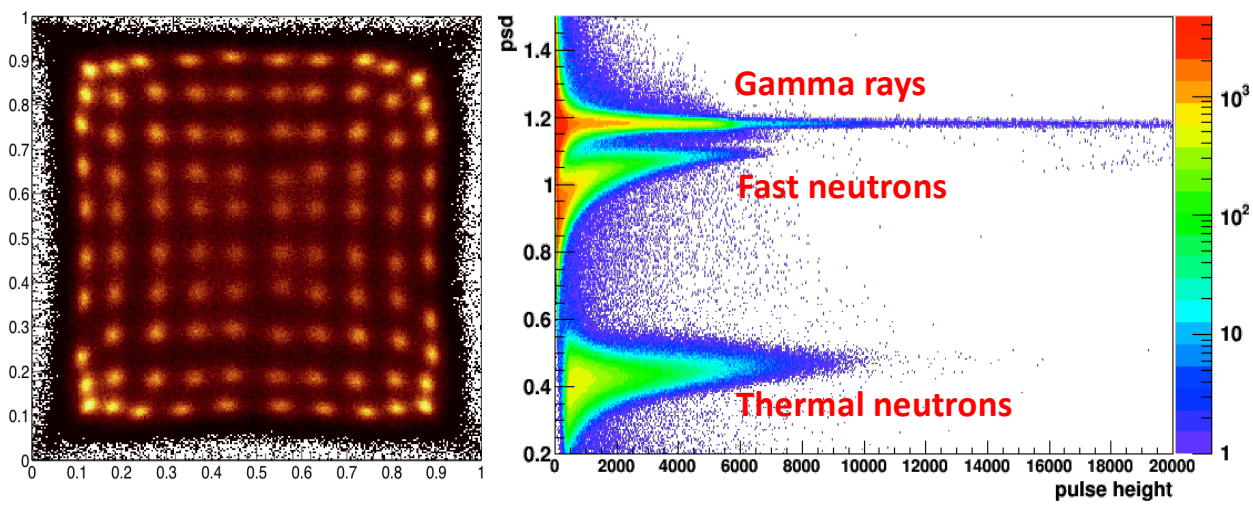

Figure 3. The (left) position response of a detector to uniform illumination by fast neutrons, and (right) pulse shape response to a combination of gamma rays, fast neutrons, and thermal neutrons.

Likewise, the shape of each pulse was calculated as a ratio of prompt to total light for the four-PMT detector sum. The PSD-plastic scintillator is sensitive to fast neutrons and gamma rays, and the additional ZnS/LiF phosphor is sensitive to thermal neutrons. The pulse shape as a function of pulse height is shown on the right of Figure 3 for a large number of pulses when the detector was illuminated by a moderated ^{241}Am(Be) source, and the contributions of gamma rays, fast neutrons, and thermal neutrons are labeled. In the present work, identified fast neutrons corresponded to those signals whose shape was within two standard deviations of the mean of the fast neutron distribution (for the appropriate pulse height) and at least five standard deviations from the mean of the gamma ray distribution.

Because the PSD-plastic detectors and data acquisition were integrated into the fast-neutron imaging system, it was desirable to evaluate the detectors for active coincidence counting while keeping the imaging system largely intact. Maintaining the planar detector geometry also helped to simplify the understanding of inter-detector scattering in this first investigation. Similarly, in this initial evaluation, it

was desirable to keep the source and sample geometry identical to that used for AWCC measurements. As a result, a fixture was designed and fabricated to mount the sleeve, Cd shield, and moderator "end plugs" from the AWCC on the imager in place of the imager's mask-holder assembly. To allow the AWCC sleeve to be placed in contact with the detector panel face, a new borated polyethylene shield was fabricated that does not extend beyond the lead shielding in front of the detectors. When the AWCC sleeve was positioned in contact with the detectors, the center of the source was about 14 cm from the surface of the lead shield. A sample holder was also designed and built for repeatability in positioning the sample within the AWCC sleeve. Figure 4 shows (left) a drawing of the AWCC sleeve mounted in front of the PSD-plastic detector panel of the imager and (right) a cutaway of the AWCC sleeve showing the sleeve, polyethylene and plugs and ^{241}Am(Li) sources, sample holder, and sample. Note the sample holder was dropped into the lower ^{241}Am(Li) plug and was constrained when the upper plug was put in place. The top ring on the sample holder was loosened to change or remove the sample prior to switching source standards. Similarly, Figure 5 shows a photograph of the AWCC sleeve mounted on the imager, ready for measurement.

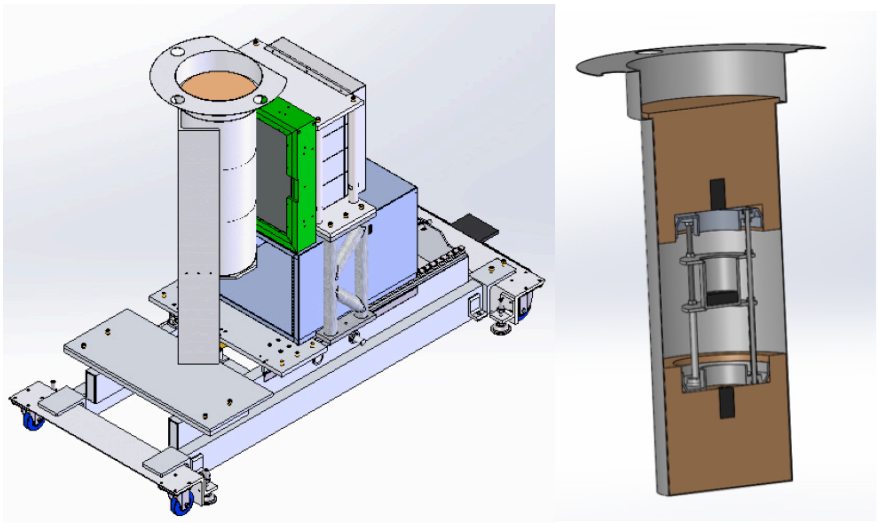

Figure 4. The imager with the source holder designed specifically for this work, and (right) a cutaway of the sleeve showing the sleeve, the ^{241}Am(Li) plugs, and the mounting of the sources internal to the sleeve.

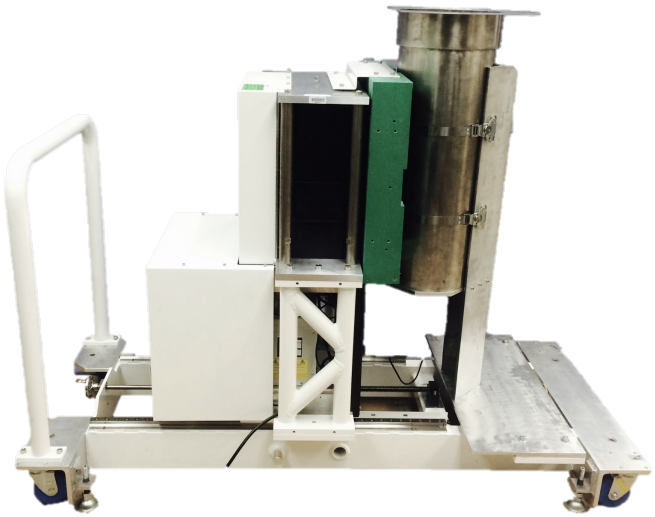

Figure 5. Photograph of the AWCC sleeve mounted in front of the PSD-plastic detector panel.

For this geometry, we estimated the singles and doubles efficiency for fission spectra neutrons to plan a series of measurements of ^{235}U standards with masses ranging from 0.52 g to 181.15 g.

4. PROOF OF PRINCIPLE MEASUREMENTS

The fast-neutron well counter evaluation configuration was characterized through a series of ^{241}Am(Be) and ^{252}Cf measurements to understand the effects of finite detector segmentation and fast-neutron multiple scattering. Following these measurements, a series of uranium standards having ^{235}U masses ranging from 0.52 g to 181.15 g were measured.

4.1 DETECTOR CHARACTERIZATION

The fast-neutron well counter was characterized through a series of ^{252}Cf and ^{241}Am(Be) measurements. The purpose of these measurements was to understand the efficiency of the detector panel (for neutron singles and doubles), as well as the effects of finite detector segmentation and fast-neutron multiple scattering.

Prior to the measurements, calculations were performed to estimate the efficiency of the fast neutron detector panel to fission neutrons originating throughout the volume encompassed by the AWCC sleeve. These estimates were performed using an analytical expression for the solid angle of each detector face and an intrinsic detector efficiency of 0.18, and were useful for predicting rates, as well as for having an appreciation for the non-uniformity associated with a single-sided detector. Because inter-detector scatter is expected to be largely between neighboring detectors, the doubles efficiency was calculated for non-adjacent detectors. A map of the singles efficiency and non-adjacent doubles efficiency for the fast neutron detector panel is shown in Figure 6. The white circle indicates the approximate location of the AWCC sleeve.

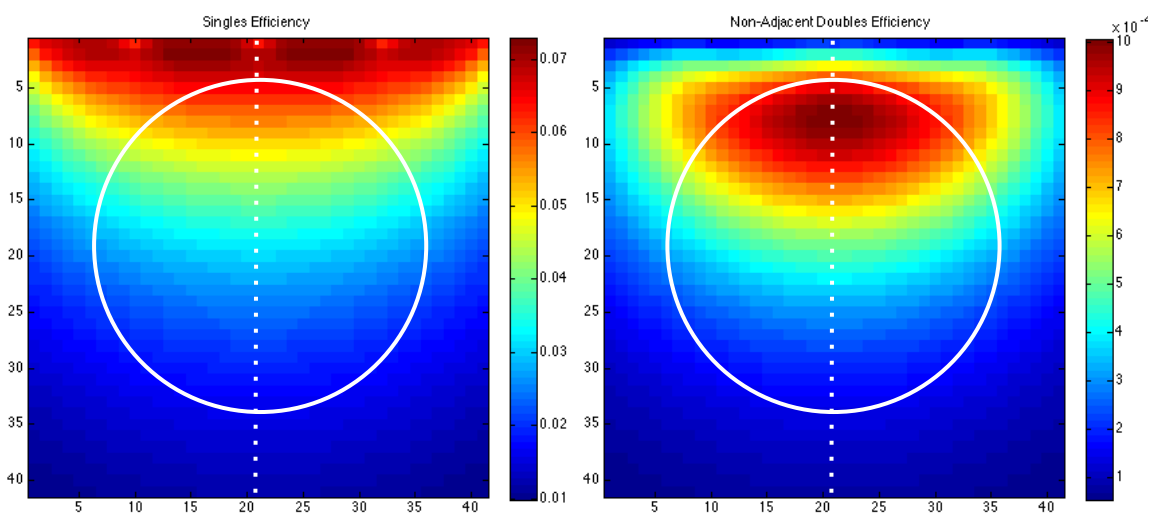

Figure 6. Estimated singles and non-adjacent doubles efficiencies based on detector solid angle and an intrinsic efficiency of 0.18.

Eleven measurements were performed using a ^{252}Cf fission source at a number of positions from the face of the detector to approximately 30 cm away along the normal to the detector at its center. This trajectory is shown on Figure 6 by the dotted white line. The calculated and measured values for the (left) neutron singles and (right) non-adjacent neutron doubles are shown in Figure 7. Note that the singles efficiency does not increase in proportion to the calculated solid angle as the source is moved closer to the detector. This smaller increase is due to coincidence summing of gamma rays and neutrons from the same fission.

As the source is moved closer to the detector, the likelihood that a gamma ray and neutron from the same fission will be detected in the same detector increases. This gamma-neutron pileup event will not normally be attributed as a neutron but somewhere between a gamma and a neutron. As a result, it does not contribute to the measured efficiency. The blue line on the plot on the left of Figure 7 shows an estimate of the expected diminution of singles efficiency due to coincidence summing (assuming a gamma ray efficiency of 0.06 and multiplicity of 7). The solid angle calculation appears to estimate the non-adjacent doubles efficiency well, but a correction factor for gamma ray pileup has not been applied. However, it is worth noting that coincidence summing will have to be accounted for when optimizing well counter design.

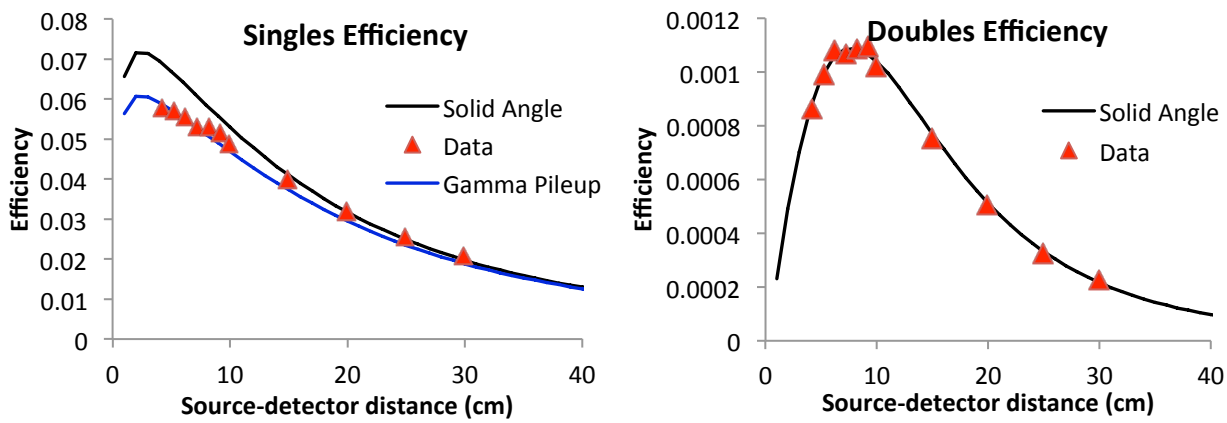

Figure 7. Comparison of measured and calculated (left) singles and (right) non-adjacent doubles efficiencies. The singles measurements indicate that at close distances there is noticeable loss in efficiency due to coincidence summing with fission gamma rays.

Subsequently, measurements with an ^{241}Am(Be) source were used to characterize fast-neutron multiple scattering. For these measurements, the ^{241}Am(Be) source was placed at the source position of the AWCC sleeve. Graphically, the character of neutron multiple scattering can be seen by looking at the hit pattern of neutron singles and neutron doubles when measuring this source. Because neutrons are emitted singly, the instances of neutron doubles originate from scattering. In Figure 8, a comparison of (left) singles to (right) scatter doubles illustrates that most of the scattering took place along the boundaries of detectors, as one would expect.

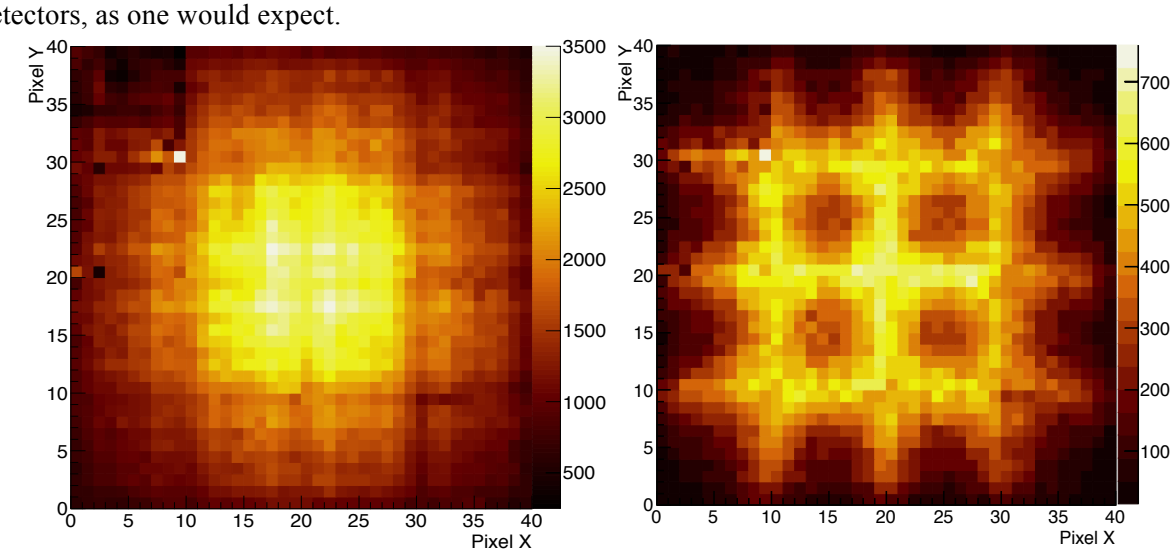

Figure 8. The distributions of (left) neutron singles and (right) neutron-scatter doubles for an ^{241}Am(Be) source positioned at the middle of the AWCC sleeve.

Since the distance between neutron hits was important, identified fast-neutron coincidences were sorted as a function of separation in time and distance in detector pixels, where 1 pixel = 1.08 cm. The ^{241}Am(Be) coincidence distribution binned in distance and in time difference is shown in the upper left in Figure 9. This distribution is dominated by the multiple scattering of fast neutrons, and it populates the bins around a trajectory of approximately 1.1 cm/ns. The same distribution was measured for a ^{252}Cf fission source that has coincidence contributions primarily from correlated fission emissions but also a minor contribution from multiple scattering of fission neutrons. To estimate the contribution from multiple scattering, the ^{241}Am(Be) distribution was scaled and subtracted from the ^{252}Cf distribution. Because the neutrons from ^{241}Am(Be) are more energetic (and more likely to produce a second scatter above threshold) than the fission neutrons, we found that a pure rate scaling overestimated the multiple-scattering contribution by about a factor of two. The resultant "pure true coincidence" distribution is shown in the upper right panel of Figure 9.

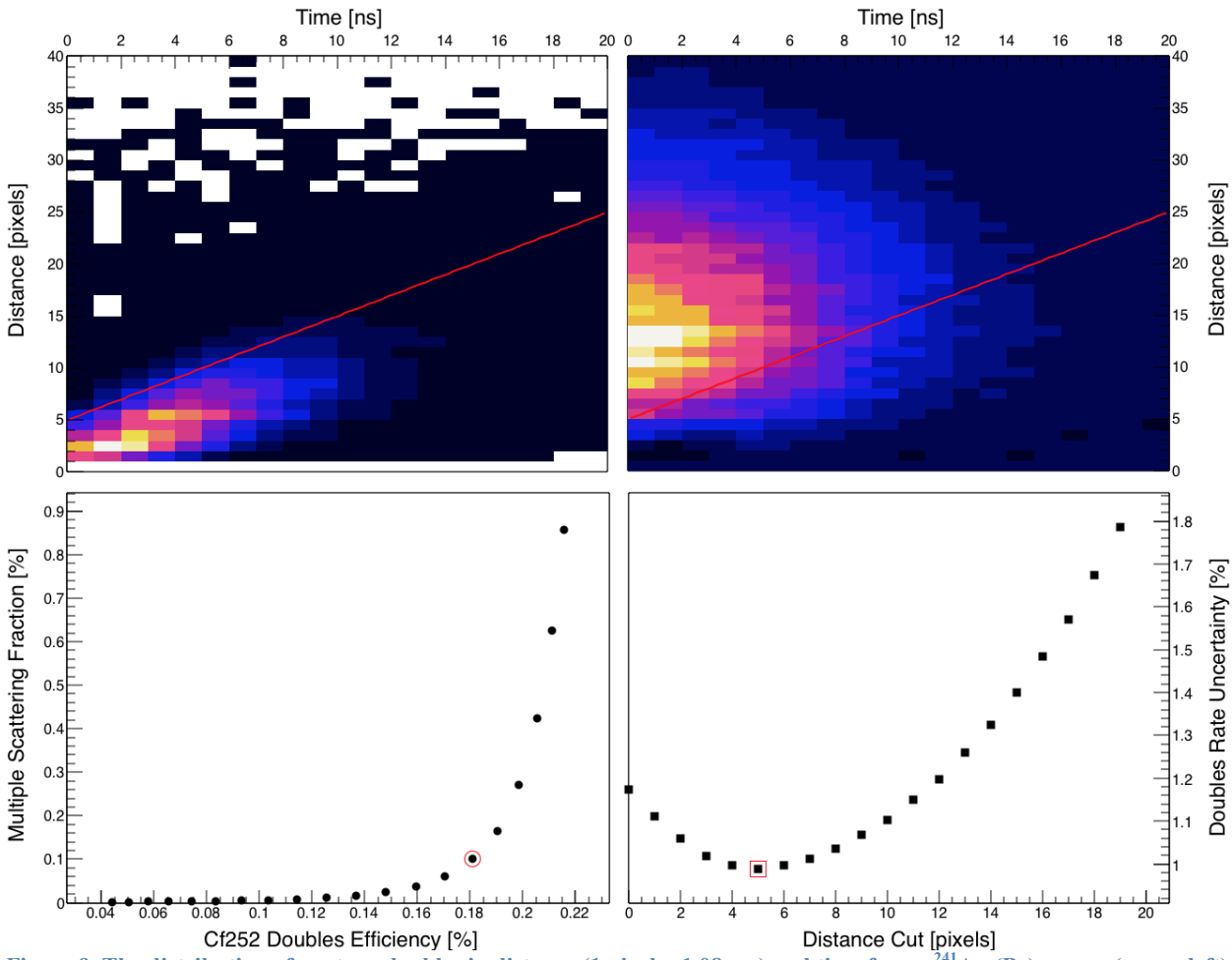

Figure 9. The distribution of neutron doubles in distance (1 pixel = 1.08 cm) and time for an ^{241}Am(Be) source (upper left) and a ^{252}Cf source (upper right) where half the rate-corrected ^{241}Am(Be) distribution is subtracted from the ^{252}Cf distribution. By accepting only doubles above the red line, the multiple scattering contribution is limited while maintaining good efficiency for fission neutron doubles. The efficiency and fraction of singles from ^{241}Am(Be) that produce a double are plotted (lower left) as the y-intercept of the cut (red line) is varied to minimize the statistical uncertainty for the largest mass (lower right).

To discriminate between scattering and true fission doubles, a linear cut (shown as a red line) in this 2D space was naturally suited to separate the multiple scatters from the true fission coincidences. The intercept in distance was varied to evaluate the compromise between efficient detector of true neutron

pairs and efficient rejection of scatter coincidences. The efficiency for measuring multiple scatters is shown as a function of the efficiency for measuring true coincidences on the lower left panel of Figure 9. Likewise, the relative uncertainty in the true coincident rate is shown as a function of the intercept of the discrimination line on the lower right panel of Figure 9. This plot, calculated for a 181-g ^{235}U standard, has the statistical uncertainty minimized for a distance intercept of 5.4 cm. With this selection, the fission doubles efficiency is estimated at $\eta\epsilon_F^2 = 0.0018$, and the average number of multiple scatters per fission neutron is $\rho_F = 0.001$. Note that using this distance-time cut increases the efficiency for fission neutron coincidences by more than a factor of two compared to the simplest possible cut of suppressing nearest neighbors. As such, the segmented detectors outperform monolithic detectors of the same size. The measured single neutron efficiency from the ^{252}Cf measurement was $\epsilon_F = 0.0510$; this efficiency includes double counting of some neutrons, so it exceeds the curve shown on the left of Figure 7. This efficiency implies a value of $\eta = 0.71$. Although this value is similar to that of the AWCC, here it is dominated by excluding coincidence counts with too small a separation rather than inefficiency of the coincidence gate of width *G* as for the AWCC. For the fast mode configuration (which will be described in the upcoming section), we find the efficiency for detection of an interrogating neutron to be $\epsilon_\alpha = 0.000945$ and the average number of multiple scatters from each interrogation neutron to be $\rho_\alpha = 0.00036$ (about a third the value for fission energies). For comparison, the doubles efficiency of the AWCC for fission neutrons is about $\epsilon_F = 0.054$, and the efficiency for the interrogating neutrons in fast mode is $\epsilon_\alpha = 0.067$. Note that the doubles efficiency for the AWCC is approximately the same as the singles efficiency for the PSD-plastic counter, but the singles rate in the AWCC from the interrogating neutrons is 120 times higher. This results in an accidental doubles rate in the AWCC from the ^{241}Am(Li) alone of 2,788 counts per second (cps), while the accidentals rate in the PSD-plastic is negligible (10^{-4} cps).

4.2 MEASUREMENTS OF URANIUM STANDARDS

Eight uranium standards, whose enrichment in ^{235}U spanned the range from depleted (0.31%) to highly enriched (93.17%) and whose ^{235}U mass spanned the range from 0.52 g to 181.15 g, were measured. In addition, measurements were performed of ambient background and the ^{241}Am(Li) sources only. Each of the ^{235}U standards was measured in two shielding configurations: one with Cd shielding over each end plug (fast mode) and one without the Cd shielding over the end plug (slow mode). The slow mode provides a higher source coupling for smaller masses but saturates more quickly for higher masses. A compilation of the total coincidence rate, coincidence rate satisfying the 2D distance-time cut, and net coincidence rate is given for fast-mode measurements of five of the standards for which long count times were available in Table 1. Neutron coincidence rates for a range of standards and backgrounds with the PSD-plastic counter in the "fast" configuration..

Table 1. Neutron coincidence rates for a range of standards and backgrounds with the PSD-plastic counter in the "fast" configuration.

^{235}U mass (g)	Time (s)	Total coincidence rate (s^{-1})	2D cut coincidence rate- (s^{-1})	Net coincidence rate (s^{-1})	True fraction
Background	328931	0.0747	0.0318		
AmLi	258324	0.2829	0.0514	0.0000	0.000
0	258324	0.2829	0.0514	0.0000	0.000
4.99	4898.18	0.3046	0.0655	0.0136	0.208
4.99	12018.6	0.3097	0.0661	0.0150	0.227
4.99	55186.8	0.3083	0.0659	0.0157	0.238
7.54	57316.1	0.3198	0.0713	0.0214	0.300

Table 1. Neutron coincidence rates for a range of standards and backgrounds with the PSD-plastic counter in the "fast" configuration.

^{235}U mass (g)	Time (s)	Total coincidence rate (s^{-1})	2D cut coincidence rate- (s^{-1})	Net coincidence rate (s^{-1})	True fraction
39.1	33438.2	0.4268	0.1361	0.0826	0.607
101.72	49999.5	0.5922	0.2331	0.1767	0.758
181.15	48716.5	0.7559	0.3280	0.2698	0.823
181.15	1800.01	0.7317	0.3139	0.2589	0.825
181.15	2134.88	0.6937	0.2848	0.2294	0.805

In this table, the "net coincidence rate" is the rate of coincidences satisfying the 2D cut subtracted for the rates expected for the ^{241}Am(Li) source, as well as the number of multiple scatters expected for the fission signal itself. Note that for small samples, a significant fraction of the coincidences satisfying the 2D cut originates from scatter. At present, only the statistical error associated with the subtraction is considered. The fraction of neutron singles resulting in scatter doubles is taken as known; however, small inaccuracies in this number could result in large inaccuracies in the net neutron rate for small samples.

The measured fission doubles rates and statistical uncertainties are shown for measurements in slow mode and fast mode in Figure 10. Several masses were measured multiple times and in the same mode. For the 40-g standard we achieved 2% statistical uncertainty in about 9 h in the fast mode (or about 9% in 30 min). Three points are presented for the 181-g standard in the fast mode: two for a half hour each, achieving 5% uncertainty, and one for 13 h, achieving 1% uncertainty. For the same mode and source placement, the AWCC achieved 0.54% uncertainty in 80 h, which corresponds to about 6.8% in half an hour. For the range of masses measured here, the PSD-plastic system already outperforms the AWCC for the following reasons. The dominant source of uncertainty in the AWCC is the accidentals doubles rate (about four-fifths of the total uncertainty for the largest mass), but for the PSD-plastic system the accidentals rate is negligible and the largest source of uncertainty is the detected doubles rate itself. The estimated fission doubles rate for the PSD-plastic is only 0.26 cps, but for the AWCC the estimated fission doubles rate is about 25 cps. A factor of 31 in the doubles rate is simply due to the difference in doubles efficiency, and the remaining factor of 3.13 is attributable to increased source coupling from the reflection of the complete azimuthal instrumentation in the AWCC.

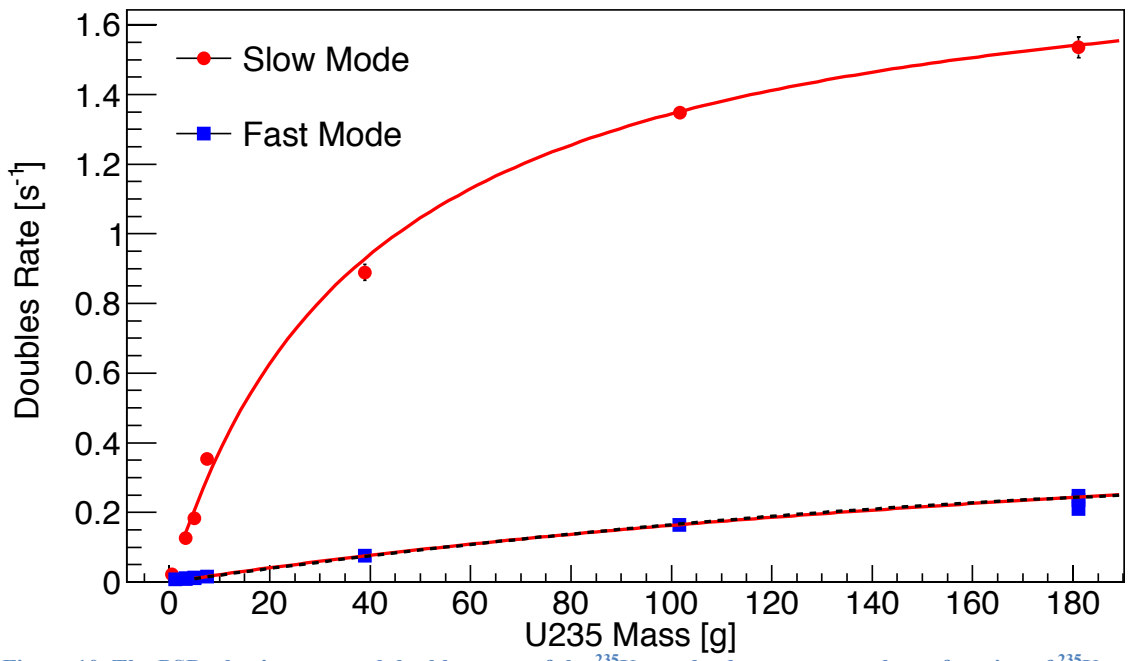

Figure 10. The PSD-plastic measured doubles rates of the ^{235}U standards are presented as a function of ^{235}U mass. A rational function of the form $D_F = Am/(1 + Bm)$ is fit to each curve. A second curve (dotted) was fit to the fast mode data and is described in the text.

A rational function of the form $D_F = Am/(1 + Bm)$ was fit to each data from each mode. The fit values for the slow mode are A = 0.047 and B = 0.025, and for the fast mode the values are A = 0.0022 and B = 0.0035. Note that although the slow mode has about twenty times the induced fission rate at lower masses, the saturation factor is 7 times larger. The shape of this curve is only useful for interpolation; extrapolation beyond the measured masses grossly overestimates the saturation. For the purposes of extrapolating to higher ^{235}U masses, we add a quadratic term to the numerator such that the asymptotic slope is consistent with the 0.10 cps reported for the AWCC for high enrichment metal [1]. For extrapolating the performance of the PSD-plastic proof-of-concept detector, we fit the measured data with the modified rational function but scale the asymptotic slope by a factor of 0.32 to account for the observed difference in source coupling.

4.3 PREDICTED PERFORMANCE OF THE PSD PLASTIC COMPARED TO THE AWCC

Using the measured rates and the extrapolation of source coupling, it is possible to make predictions of the present PSD-plastic counter as a function of ^{235}U mass. It is also possible to predict the performance of the PSD-plastic counter where it has been reconfigured to increase its efficiency or to increase the rate of interrogation. For example, if the detectors of the fast-neutron imager panel were reconfigured as shown in Figure 11, this change would increase the neutron efficiency by a factor of approximately 4 and would increase the doubles efficiency by a factor of 16. Since the multiple scattering of fast-neutrons only contributes about 7% to the doubles rate for the largest measured mass and scales with the singles rate, the number of total doubles will remain the dominant uncertainty on the estimate of fission doubles. The reconfigured geometry will also increase the source coupling from reflections of the full azimuthal instrumentation to match more closely the coupling of the AWCC. Furthermore, with a coincident gating window thousands of times smaller than the AWCC, measurement times could be dramatically reduced by increasing the fission rate with a higher activity neutron source. The combined neutron and gamma

rate in the proof-of-concept detector was about 8000 kHz with the two 5×10^4 neutrons·s^{-1} sources. The neutron source could be increased by a factor of 10 without compromising the identification of neutrons with pulse shape discrimination. Together these factors would allow the system to reach the same statistical significance in one 160th of the time.

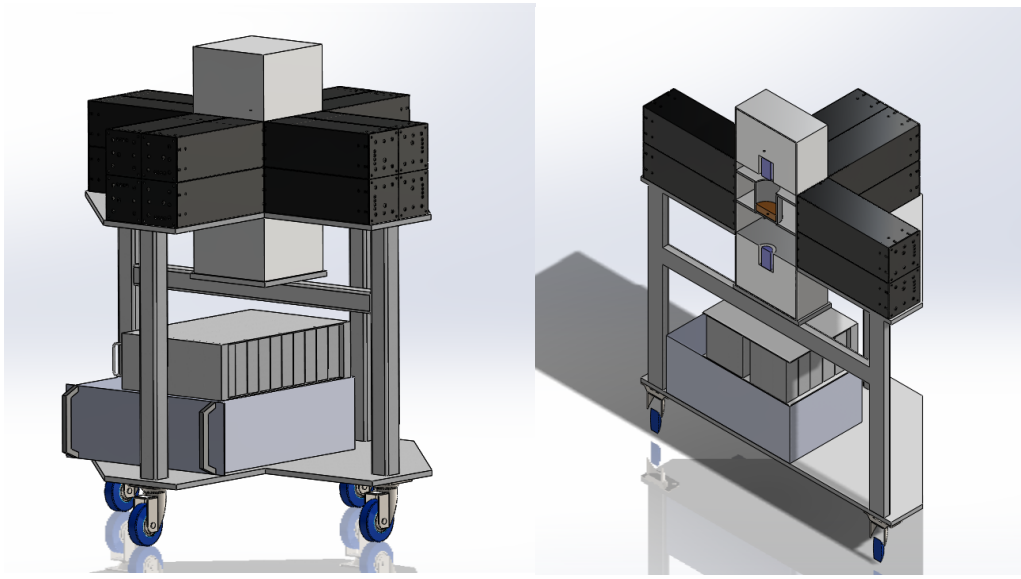

Figure 11. Proposed Reconfigured Detector.

We predict the performance of the proof-of-concept detector and the reconfigured detector for ^{235}U masses up to 8 kg in Figure 12. The predicted performance of the reconfigured detector uses the source coupling inferred from the doubles rate (0.10 cps) reported for the AWCC for large masses. The predicted measurement precision is shown for 60- and 600-s dwell times as a function of ^{235}U mass for the AWCC, the proof-of-concept PSD-plastic detector, and the reconfigured PSD-plastic detector. Note that the proof-of-concept PSD-plastic system outperforms the AWCC for masses less than 550 g, above which the AWCC doubles efficiency provides the advantage. For the proposed reconfigured system, the increased efficiency allows for a 5% statistical uncertainty measurement for all ^{235}U masses above 72 g in approximately 60 s and 3% statistical uncertainty measurement for all masses above 275 g. With a factor of 10 increase in the induced fission rate, we achieve 5% and 3% precision for 5 g and 15 g, respectively, in 60 s. In 600 s, 3% precision is achieved for 1.6 g.

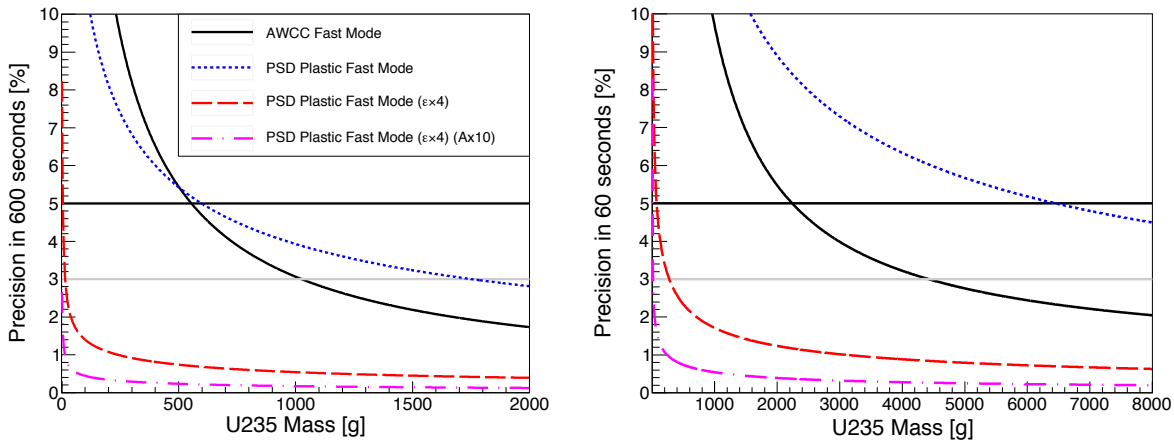

Figure 12. The performance of the AWCC and PSD-plastic operated in "fast mode" with two interrogating sources in each end plug each with activity of 5×10^4 neutrons·s^{-1}. Also, shown is the predicted performance for a reconfigured PSD-plastic system with four times the singles efficiency and with interrogating activities scaled by a factor of 10.

The relative error in a 600-s measurement can also be shown as a function of the interrogating ^{241}Am(Li) source strength. This is plotted in Figure 13 for the 181-g ^{235}U sample and the (black) AWCC, (blue dotted) PSD-plastic panel, and (red dashed) PSD-plastic well geometry. Note that the dashed grey line indicates the present strength of the source. Note that increasing the source intensity an order of magnitude leaves the performance of the AWCC unchanged, but improves the performance of the PSD-plastic detectors by more than a factor of three.

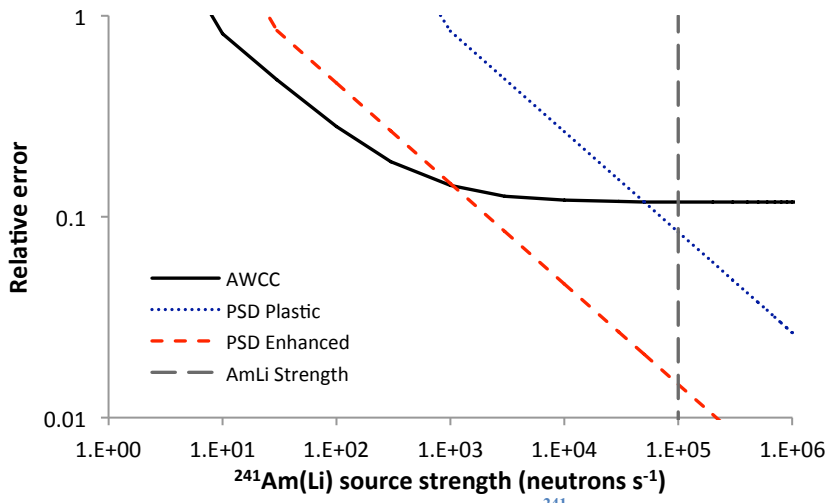

Figure 13. The relative error as a function of the ^{241}Am(Li) source strength.

5. MULITPLE-SCATTERING SYSTEMATICS

For the PSD-plastic counter, multiple scattering doubles are the single largest background to the doubles distribution. The analysis procedure described in Section 2 assumes that the rate of scatter doubles from the source when a sample is present is the same as that measured when the sample is absent. Then, the rate of scatter doubles due to the sample is calculated by multiplying the increase in singles rate due to the sample by the estimated scatter double probability inferred from a ^{252}Cf measurement. This prescription assumes that the presence of the sample does not alter the rate from the ^{241}Am(Li) source or the

probability that a neutron scatters and is detected more than once. This method is deterministic, making it straightforward to propagate statistical errors to predict performance as described in Section 4.3, and likely quite reasonable for samples similar in mass and bulk to the calibration standards. However, the large rate of scatter doubles and the considerable dependence of the scatter probability on the neutron spectrum (the rate of production of scatter doubles from neutron singles varies by a factor of 8 between the ^{241}Am(Li) and ^{241}Am(Be) sources) suggest that this subtraction could have substantial systematic errors. Moreover, for counters constructed from PSD plastic to also be useful for counting plutonium, it is necessary to be able to infer the number of true and scatter doubles from the data without a priori knowledge of the fraction of neutrons originating from fission and from (α,n) reactions.

In general, the number of multiple scattering doubles scales like the number of single neutron detections. However, the fraction of detected neutrons that scatter and are detected again depends on the energy distribution of the neutrons. For instance, we find that on average, a detected neutron from an ^{241}Am(Be) source is almost eight times more likely to be detected twice than a neutron detected from an ^{241}Am(Li) source. The pulse height distributions corresponding to neutron detection in the PSD-plastic detectors for neutrons originating from ^{241}Am(Be), ^{241}Am(Li), and ambient background are presented in Figure 14.

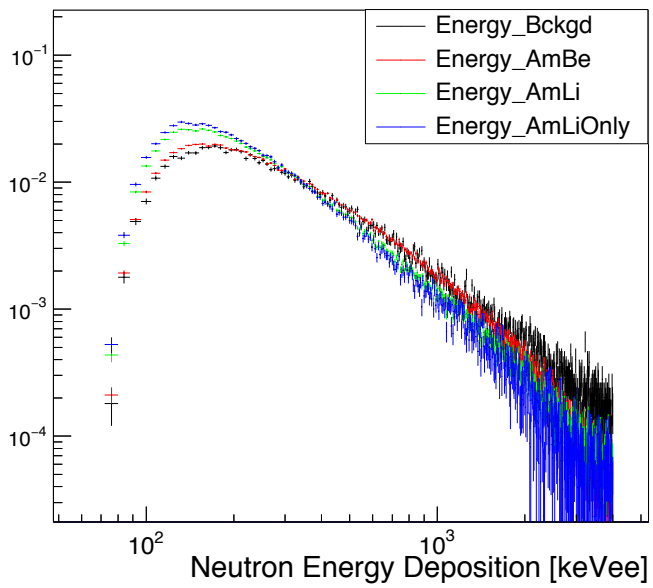

Figure 14. Energy deposition distribution for Backgrounds, Am(Be), AmLi(+Bckgd), and AmLi Only.

One approach is to estimate the input neutron energy spectrum from the detected pulse height spectrum, and then estimate the expected scatter doubles for that energy distribution via simulations. In the future, it would be desirable to perform simulations to build the detector response as a function of input in energy to make the aforementioned estimate.

However, an alternative approach is to use the normalized spatial and time difference distributions for fissions (measured for ^{252}Cf) and for scattered neutron doubles [measured for ^{241}Am(Li) and ^{241}Am(Be) sources] to fit the distributions of unknown samples to a sum of fissions and scatters. In this case, the fit values give the numbers of fission and scatter doubles. This prescription was executed separately using the scattered neutron doubles distributions given by measurements of the ^{241}Am(Li) and ^{241}Am(Be) sources. To identify the distribution based on the ^{241}Am(Li) source alone, the ambient background was subtracted. Using this approach, the extracted number of fission doubles and scatter doubles was independent of the source used for the scatter distribution. This procedure allowed us to estimate the total contribution of fission doubles. To compare it to the previous estimates of coincident neutrons obtained

by subtraction, it is necessary to apply the 78% efficiency of the 2D spatial-time distance cut described in Section 4.1. The spatial and time difference distributions for (left) ^{241}Am(Be), (middle) ^{241}Am(Li), and (right) ^{252}Cf are shown in Figure 15. The fit and residuals of an example measurement of the 181-g standard using the scatter doubles measured for the ^{241}Am(Be) source is shown in Figure 16, and the corresponding fit using the scatter doubles measured for the ^{241}Am(Li) source is shown in Figure 17.

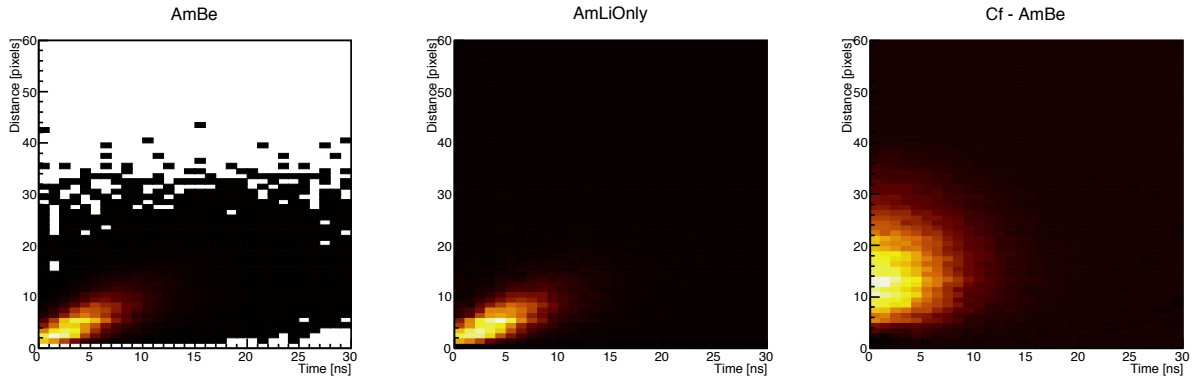

Figure 15. The doubles distributions over spatial and time separation within the detector plane for ^{241}Am(Be), ^{241}Am(Li), and ^{252}Cf. The center "AmLiOnly" plot is a subtraction of the ambient background distribution from the ^{241}Am(Li) dataset. The "Cf–AmBe" distribution is the estimated true fission doubles distribution obtained by subtracting half the single-neutron-rate scaled ^{241}Am(Be) distribution from the ^{252}Cf distribution.

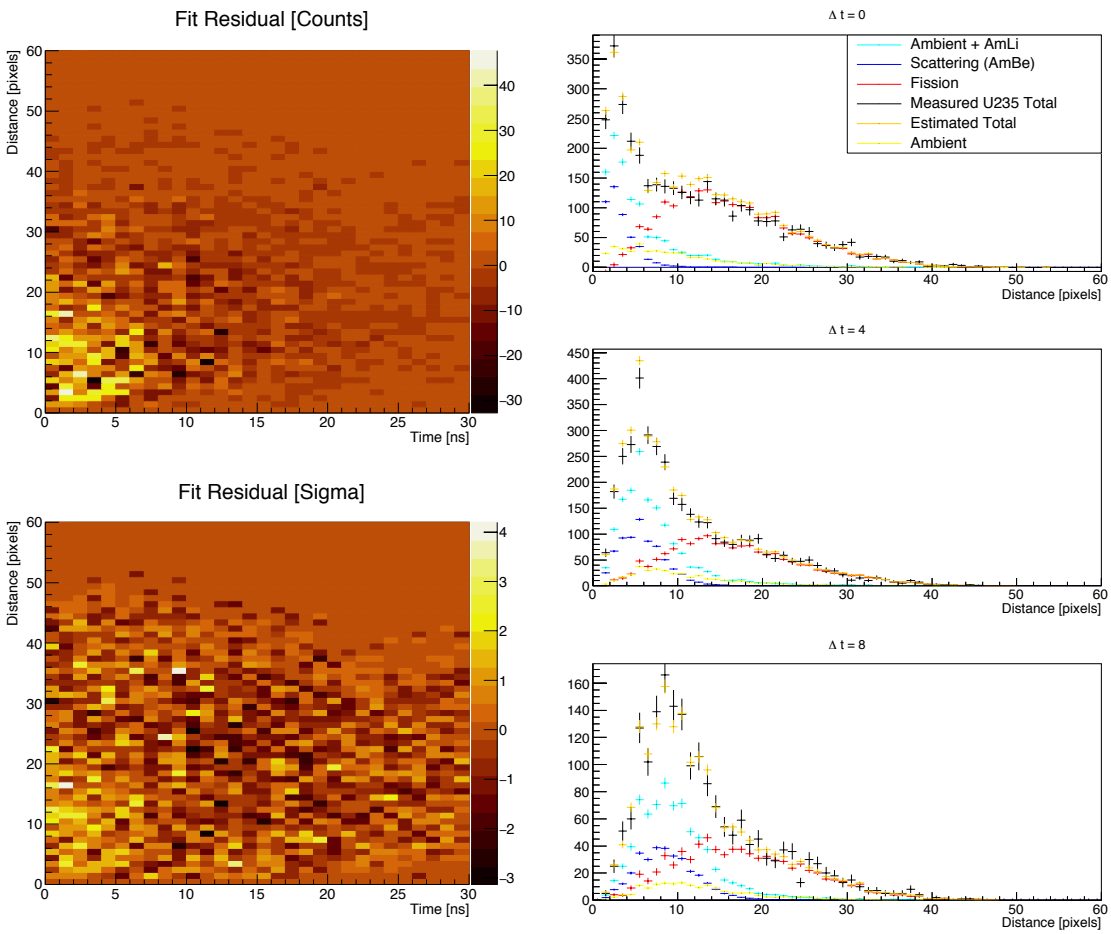

Figure 16. The doubles distribution collected for 13.5 h of 181 g of ^{235}U is fit by subtracting the duration scaled Ambient+AmLi distribution and the fission (Cf-AmBe) distribution, and multiple-scattering [^{241}Am(Be)] distributions are allowed to vary. The 2D residuals (in counts and sigma) are shown on the left, and three slices in time-difference of the distributions are shown on the right.

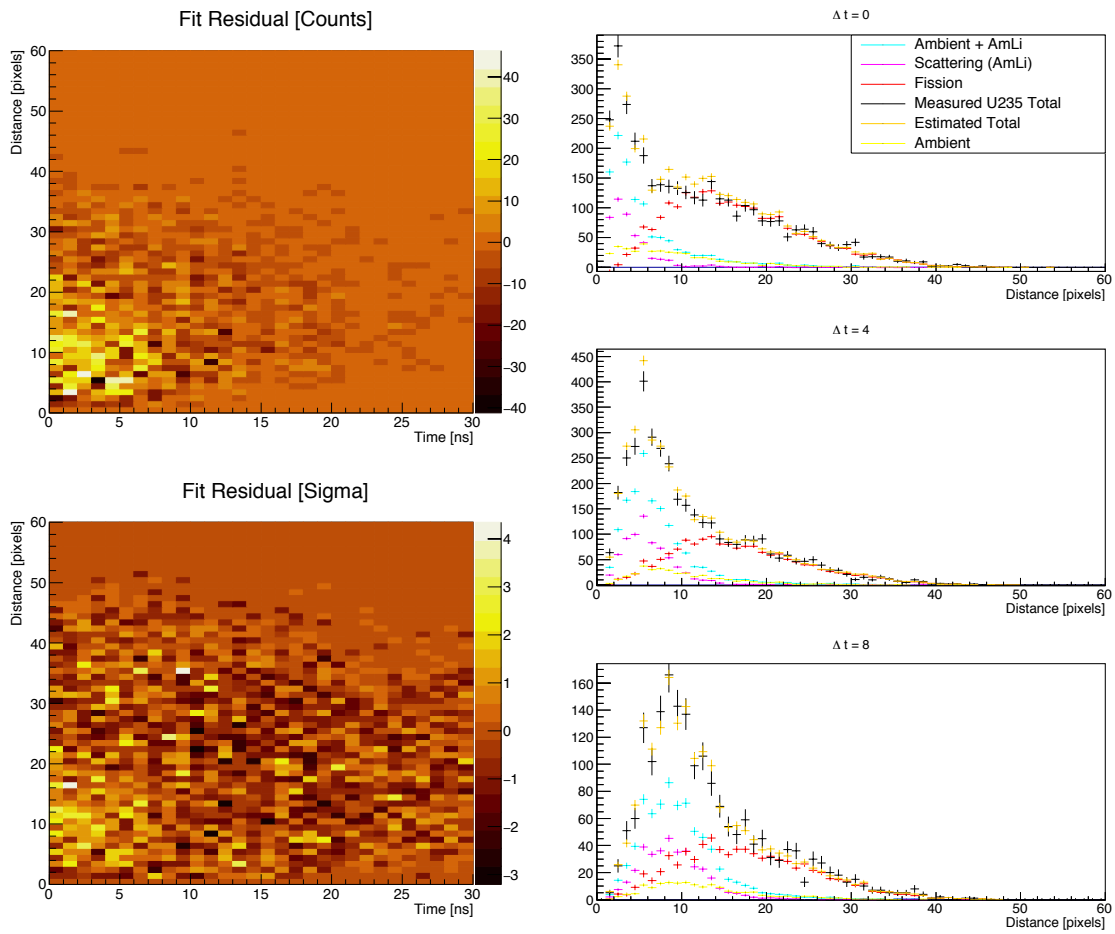

Figure 17. The doubles distribution collected for 13.5 h of 181 g of ^{235}U is fit by subtracting the duration scaled Ambient+AmLi distribution and the fission (Cf-AmBe) distribution, and multiple-scattering [^{241}Am(Li)] distributions are allowed to vary. The 2D residuals (in counts and sigma) are shown on the left, and three slices in time-difference of the distributions are shown on the right.

Last of all, in Figure 18, the values from the fits of all measurements were compared to the values previously estimated using the 2D spatial-time difference cut. In the upper panel of Figure 18, the values extracted for both methods are plotted as a function of ^{235}U mass. In the lower panel, the values are shown where the rational function shown by the yellow line has been subtracted.

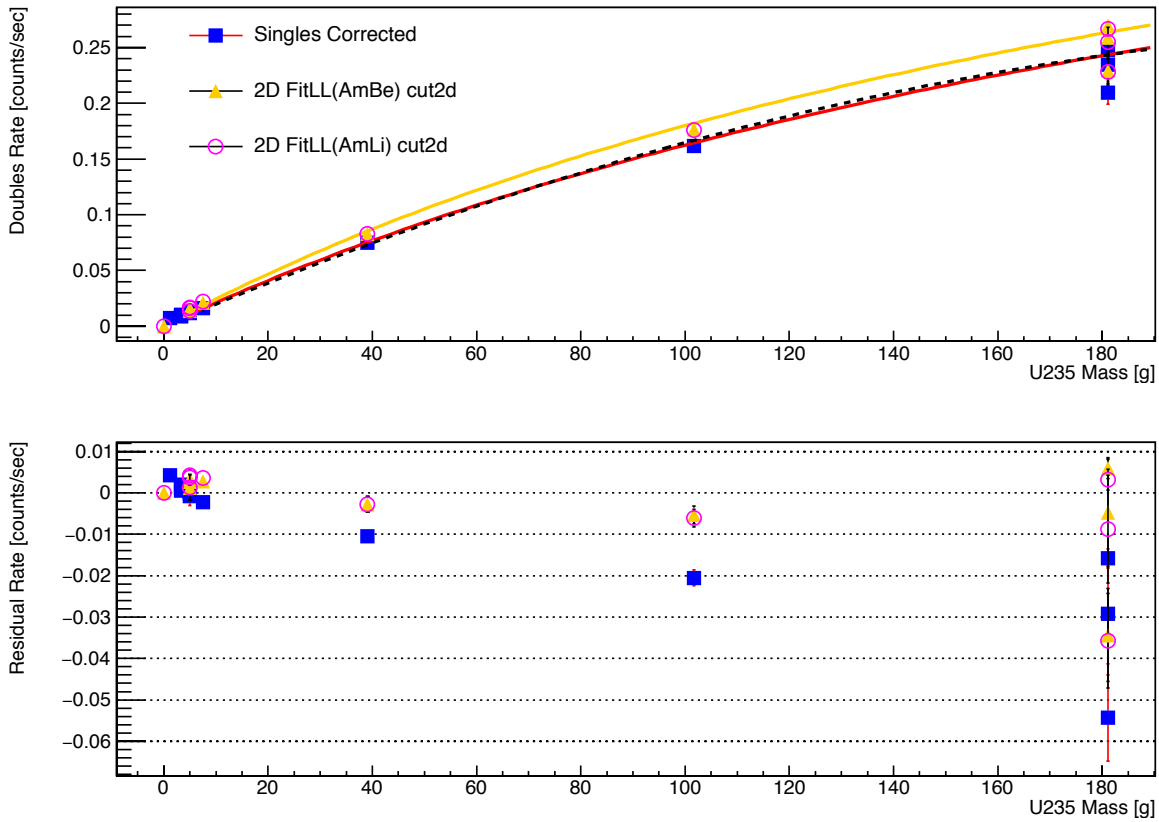

Figure 18. Comparison of the corrected doubles rate with the doubles rate from fitting the 2D doubles distributions.

6. SUMMARY

In the present work, we evaluated an existing array of PSD-plastic detectors for the purposes of quantifying bulk uranium. The detector array used a data acquisition approach composed of off-the-shelf free-running waveform digitizers in a well-established chassis format. To the extent that was reasonable, data were written to disk in a raw format that enabled detailed offline analysis that could be updated as analysis techniques improved. Remarkably, the performance of this existing, non-optimized, single detector slab approximately equaled the performance of the traditional AWCC system. Moreover, a coincidence counter composed of multiple PSD-plastic detectors in an optimized geometry will far exceed the measurement performance of the AWCC, enabling either significantly reduced assay times or increased precision. The fast-neutron detector assemblies also provide additional information related to timing, pulse height distributions, and coincidence multiplicities that may afford improved accuracy to identify unexpected material configurations.

7. REFERENCES

[1] H.O. Menlove, *Description and Operation Manual for the Active Well Coincidence Counter*, LA-7823-M, Los Alamos National Laboratory, May 1979.

[2] J. Newby, P. A. Hausladen, M. A. Blackston, J. F. Liang, *Performance of Fast Neutron Imaging Detectors Based on Plastic Scintillator EJ-299-34*, ORNL/TM-2013/82, UT-Battelle, LLC, Oak Ridge National Laboratory, 2013.

[3] M. A. Blackston, B. L. Brown, E. Brubaker, L. Fabris, P. A. Hausladen, P. Marleau, and J. Newby, "Fast Neutron Coded-Aperture Imaging for Warhead Counting," 52nd Annual Meeting of the Inst. of Nucl. Materials Mgmt., 2011.

[4] P. A. Hausladen, M. A. Blackston, E. Brubaker, D. L. Chichester, P. Marleau, and R. J. Newby, "Fast-Neutron Coded-Aperture Imaging of Special Nuclear Material Configurations," 53nd Annual Meeting of the Inst. of Nucl. Materials Mgmt., 2012.